

Solid electrolytes for battery applications – a theoretical perspective*

N. A. W. Holzwarth**

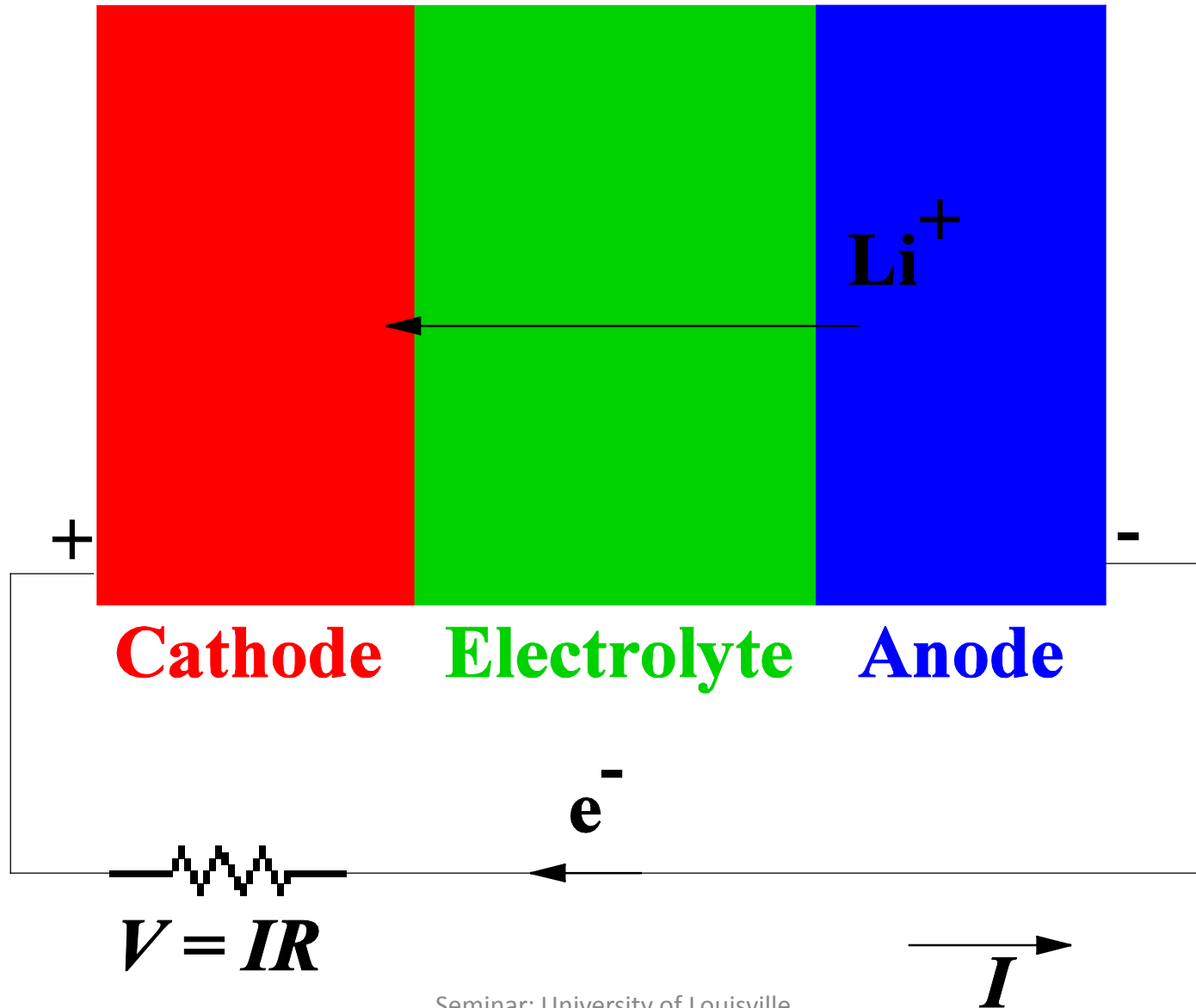
Wake Forest University, Winston-Salem, NC, USA, 27109

- Motivation and background information
- Overview of computational methods
- Some representative results

*Supported by NSF Grants DMR-0705239 and DMR-1105485.

**With help from Nicholas Lepley (graduate student) and previously, Yaojun Du (postdoc).

Materials components of a Li ion battery



Example: Thin-film battery developed by Nancy Dudney and collaborators at Oak Ridge National Laboratory – **LiPON** (lithium phosphorus oxinitride)

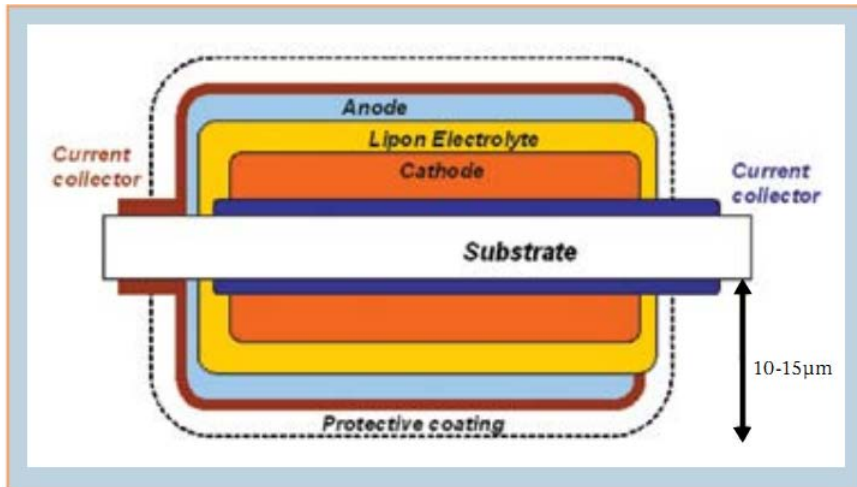


FIG. 1. Schematic cross section of a thin film battery fabricated by vapor deposition onto both sides of a substrate support.

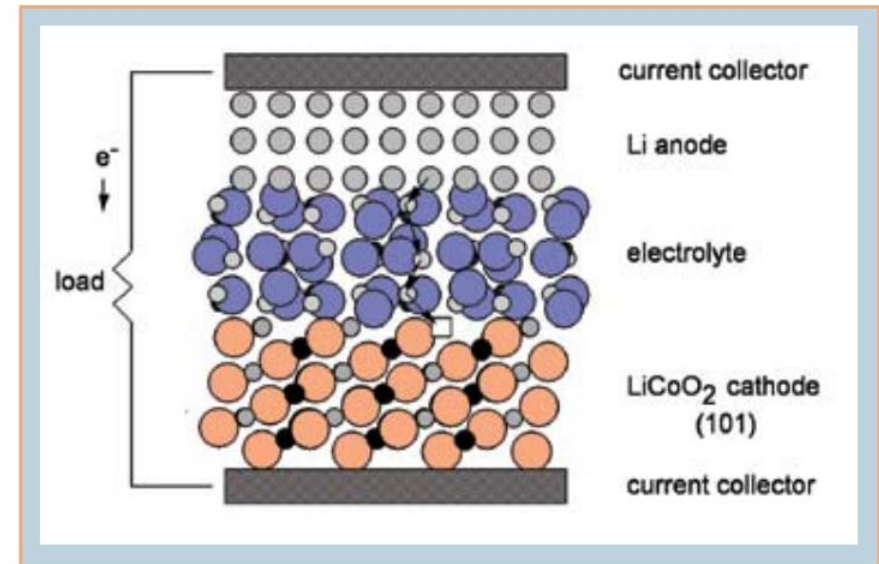


FIG. 2. Schematic illustration of a thin film battery. The arrows indicate the discharge reaction where a Li ion diffuses from the lithium metal anode to fill a vacancy in an intercalation compound that serves as the cathode. The compensating electron is conducted through the device.

From: N. J. Dudney, *Interface* **77**(3) 44 (2008)

Solid vs liquid electrolytes in Li ion batteries

Solid electrolytes

Advantages

1. Excellent chemical and physical stability.
2. Perform well as thin film ($\approx 1\mu$)
3. Li^+ conduction only (excludes electrons).

Disadvantages

1. Reduced contact area for high capacity electrodes.
2. Interface stress due to electrode charging and discharging.
3. Relatively low ionic conductivity.

Liquid electrolytes

Advantages

1. Excellent contact area with high capacity electrodes.
2. Can accommodate size changes of electrodes during charge and discharge cycles.
3. Relatively high ionic conductivity.

Disadvantages

1. Relatively poor physical and chemical stability.
2. Relies on the formation of “solid electrolyte interface” (SEI) layer.
3. May have both Li^+ and electron conduction.

Motivation: Paper by N. Kayama, *et. al* in **Nature Materials** **10**, 682-686 (2011)

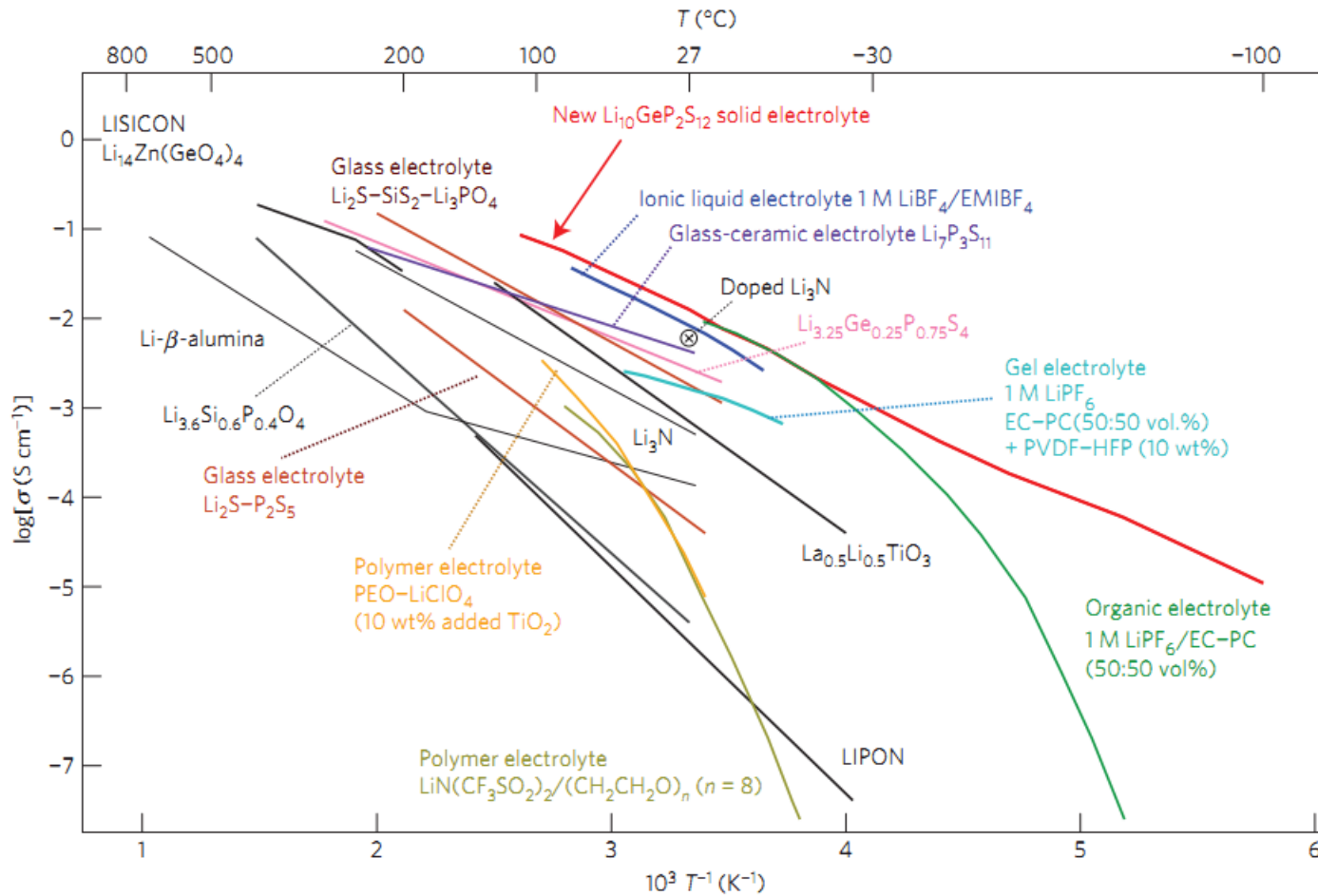


Figure 3 | Thermal evolution of ionic conductivity of the new $\text{Li}_{10}\text{GeP}_2\text{S}_{12}$ phase, together with those of other lithium solid electrolytes, organic liquid electrolytes, polymer electrolytes, ionic liquids and gel electrolytes^{3-8,13-16,20,22}. The new $\text{Li}_{10}\text{GeP}_2\text{S}_{12}$ exhibits the highest lithium ionic conductivity (12 m S cm^{-1} at $27 \text{ }^{\circ}\text{C}$) of the solid lithium conducting membranes of inorganic, polymer or composite systems. Because organic electrolytes usually have transport numbers below 0.5, inorganic lithium electrolytes have extremely high conductivities.

Motivation: Paper by N. Kamaya, *et. al* in *Nature Materials* **10**, 682-686 (2011)

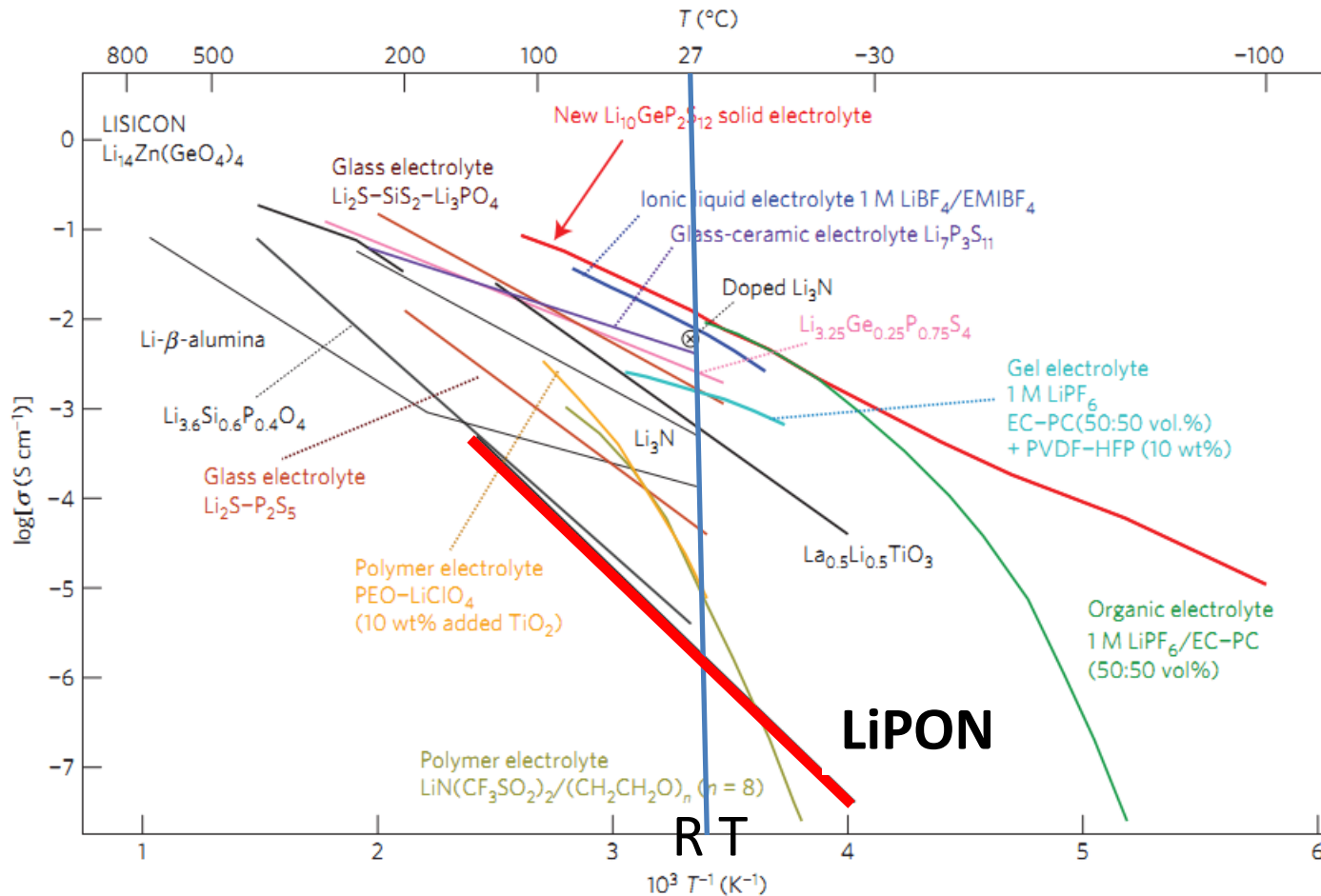


Figure 3 | Thermal evolution of ionic conductivity of the new $\text{Li}_{10}\text{GeP}_2\text{S}_{12}$ phase, together with those of other lithium solid electrolytes, organic liquid electrolytes, polymer electrolytes, ionic liquids and gel electrolytes^{3-8,13-16,20,22}. The new $\text{Li}_{10}\text{GeP}_2\text{S}_{12}$ exhibits the highest lithium ionic conductivity (12 m S cm^{-1} at 27°C) of the solid lithium conducting membranes of inorganic, polymer or composite systems. Because organic electrolytes usually have transport numbers below 0.5, inorganic lithium electrolytes have extremely high conductivities.

Motivation: Paper by N. Kamaya, *et. al* in **Nature Materials** **10**, 682-686 (2011)

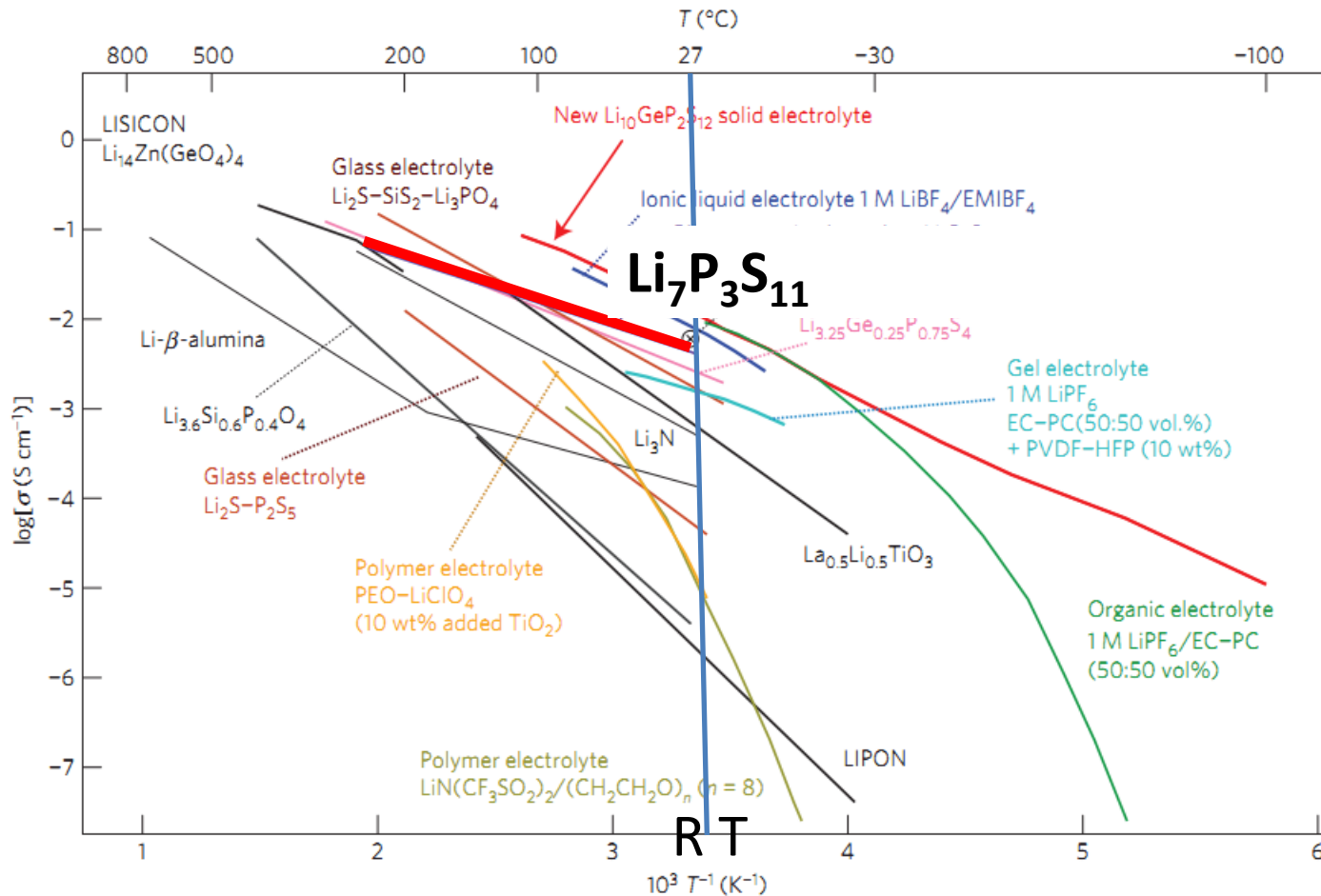


Figure 3 | Thermal evolution of ionic conductivity of the new $\text{Li}_{10}\text{GeP}_2\text{S}_{12}$ phase, together with those of other lithium solid electrolytes, organic liquid electrolytes, polymer electrolytes, ionic liquids and gel electrolytes^{3-8,13-16,20,22}. The new $\text{Li}_{10}\text{GeP}_2\text{S}_{12}$ exhibits the highest lithium ionic conductivity (12 mS cm^{-1} at 27°C) of the solid lithium conducting membranes of inorganic, polymer or composite systems. Because organic electrolytes usually have transport numbers below 0.5, inorganic lithium electrolytes have extremely high conductivities.

Motivation: Paper by N. Kamaya, *et. al* in *Nature Materials* **10**, 682-686 (2011)

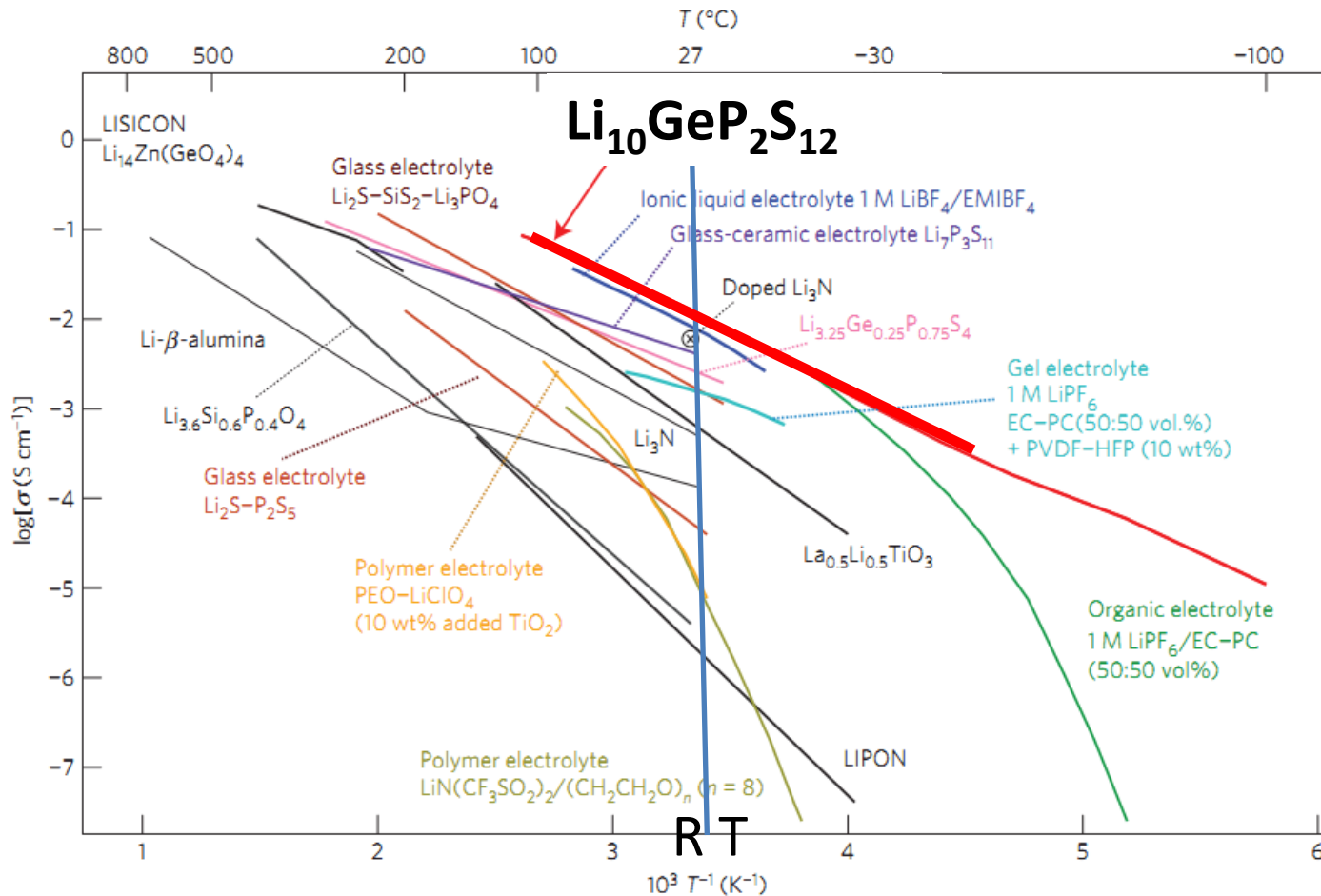


Figure 3 | Thermal evolution of ionic conductivity of the new $\text{Li}_{10}\text{GeP}_2\text{S}_{12}$ phase, together with those of other lithium solid electrolytes, organic liquid electrolytes, polymer electrolytes, ionic liquids and gel electrolytes^{3-8,13-16,20,22}. The new $\text{Li}_{10}\text{GeP}_2\text{S}_{12}$ exhibits the highest lithium ionic conductivity (12 m S cm^{-1} at 27°C) of the solid lithium conducting membranes of inorganic, polymer or composite systems. Because organic electrolytes usually have transport numbers below 0.5, inorganic lithium electrolytes have extremely high conductivities.

How can computer simulations contribute to the development of materials?

- Examine known materials and predict new materials
 - Structural forms
 - Relative stabilities
 - Analyze vibrational modes and other experimentally accessible properties
- Model ion migration mechanisms
 - Vacancy migration
 - Interstitial migration
 - Vacancy-interstitial formation energies

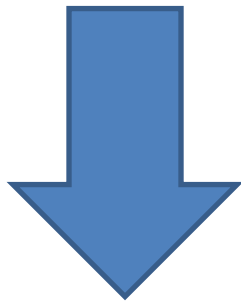
Summary of “first-principles” calculation methods

Exact problem :

$$\mathcal{H}(\{\mathbf{r}_i\}, \{\mathbf{R}^a\}) \Psi_\alpha(\{\mathbf{r}_i\}, \{\mathbf{R}^a\}) = E_\alpha \Psi_\alpha(\{\mathbf{r}_i\}, \{\mathbf{R}^a\})$$

Electronic coordinates

Atomic coordinates



Born-Oppenheimer approximation

Born & Huang, **Dynamical Theory of Crystal Lattices**,
Oxford (1954)

Density functional theory

Hohenberg and Kohn, *Phys. Rev.* **136** B864 (1964)
Kohn and Sham, *Phys. Rev.* **140** A1133 (1965)

Approximately equivalent problem :

$$\text{Ground state energy : } E_0(\mathbf{r}, \rho(\mathbf{r}), \{\mathbf{R}^a\}) \quad H_{eff}(\mathbf{r}, \rho(\mathbf{r}), \{\mathbf{R}^a\}) \psi_n(\mathbf{r}) = \varepsilon_n \psi_n(\mathbf{r})$$

$$\rho(\mathbf{r}) = \sum_n |\psi_n(\mathbf{r})|^2 \quad H_{eff}(\mathbf{r}, \rho(\mathbf{r}), \{\mathbf{R}^a\}) = \frac{\delta E_0(\mathbf{r}, \rho(\mathbf{r}), \{\mathbf{R}^a\})}{\delta \rho(\mathbf{r})}$$

More computational details:

$$H_{eff}(\mathbf{r}, \rho(\mathbf{r}), \{\mathbf{R}^a\}) = -\frac{\hbar^2 \nabla^2}{2m} + \sum_a \underbrace{\frac{-Z^a e^2}{|\mathbf{r} - \mathbf{R}^a|}}_{\text{electron-nucleus}} + e^2 \int d^3 r' \underbrace{\frac{\rho(\mathbf{r}')}{|\mathbf{r} - \mathbf{r}'|}}_{\text{electron-electron}} + \underbrace{V_{xc}(\rho(\mathbf{r}))}_{\text{exchange-correlation}}$$

Exchange-correlation functionals:

LDA: J. Perdew and Y. Wang, Phys. Rev. B **45**, 13244 (1992)

GGA: J. Perdew, K. Burke, and M. Ernzerhof, PRL **77**, 3865 (1996)

HSE06: J. Heyd, G. E. Scuseria, and M. Ernzerhof, JCP **118**, 8207 (2003)

Numerical methods:

“Muffin-tin” construction: Augmented Plane Wave developed by Slater → “linearized” version by Andersen:

J. C. Slater, Phys. Rev. **51** 846 (1937)

O. K. Andersen, Phys. Rev. B **12** 3060 (1975) (LAPW)

Pseudopotential methods:

J. C. Phillips and L. Kleinman, Phys. Rev. **116** 287 (1959) -- original idea

P. Blöchl, Phys. Rev. B. **50** 17953 (1994) – Projector Augmented Wave (PAW) method

Outputs of calculations:

Ground state energy :

$E_0(\mathbf{r}, \rho(\mathbf{r}), \{\mathbf{R}^a\}) \Rightarrow$ Determine formation energies

$\min_{\{\mathbf{R}^a\}} (E_0(\mathbf{r}, \rho(\mathbf{r}), \{\mathbf{R}^a\})) \Rightarrow$ Determine structural parameters

\Rightarrow Stable and meta - stable structures

\Rightarrow Normal modes of vibration

$\rho(\mathbf{r}) = \sum_n |\psi_n(\mathbf{r})|^2 \Rightarrow$ Self - consistent electron density

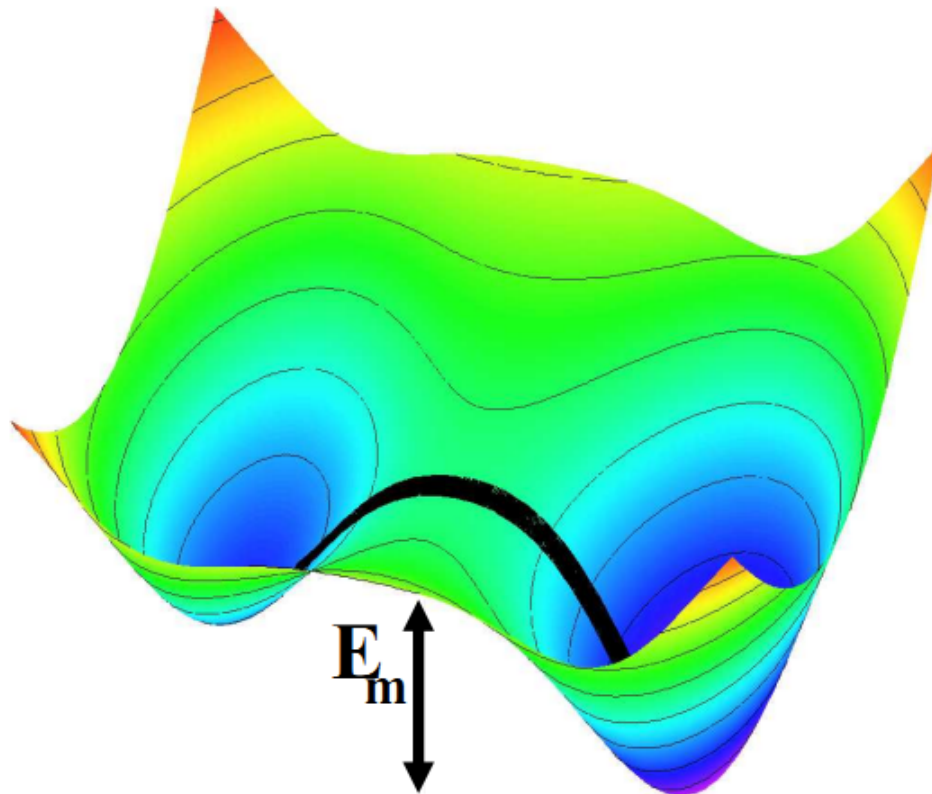
$\{\epsilon_n\}$

\Rightarrow One - electron energies; densities of states

Estimate of ionic conductivity assuming activated hopping

Schematic diagram of minimal energy path

Approximated using NEB algorithm^a
– “Nudged Elastic Band”



Arrhenius relation

$$\sigma \cdot T = K e^{-E_A/kT}$$

From: Ivanov-Shitz and co-workers,
Cryst. Reports **46**, 864 (2001):

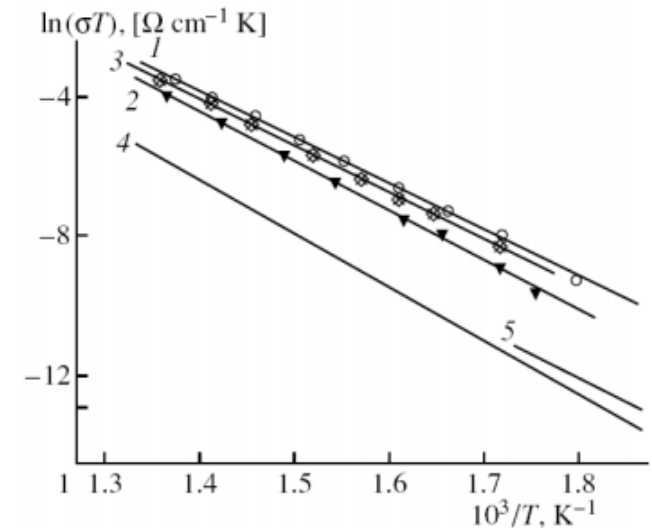


Fig. 2. Temperature dependences of conductivity in γ -Li₃PO₄: (1–3) for single crystals measured along the (1) *a*-axis, (2) *b*-axis, (3) *c*-axis and (4, 5) for a polycrystal (4) according to [4, 5] and (5) according to [7].

$E_A = 1.14, 1.23, 1.14, 1.31, 1.24$ eV for 1,2,3,4,5, respectively.

^aHenkelman and Jónsson, *JCP* **113**, 9978 (2000)

Public domain codes available for electronic structure calculations

| Method | Codes | Comments |
|--------|--|--|
| LAPW | www.wien2k.at elk.sourceforge.net | Works well for smaller unit cells; variable unit cell optimization not implemented. Need to choose non-overlapping muffin tin radii and avoid “ghost” solutions. |
| PAW | www.abinit.org www.quantum_espresso.org | Works well for large unit cells (<200 atoms or so); includes variable unit cell optimization. Need to construct and test PAW datasets |

Other efforts:

- Gerbrand Ceder’s group at MIT – Materials Project; A Materials Genome Approach -- <http://www.materialsproject.org/>
- Stefano Curtarolo’s group at Duke – Energy Materials Laboratory -- <http://materials.duke.edu/>

Code for generating atomic datasets for PAW calculations

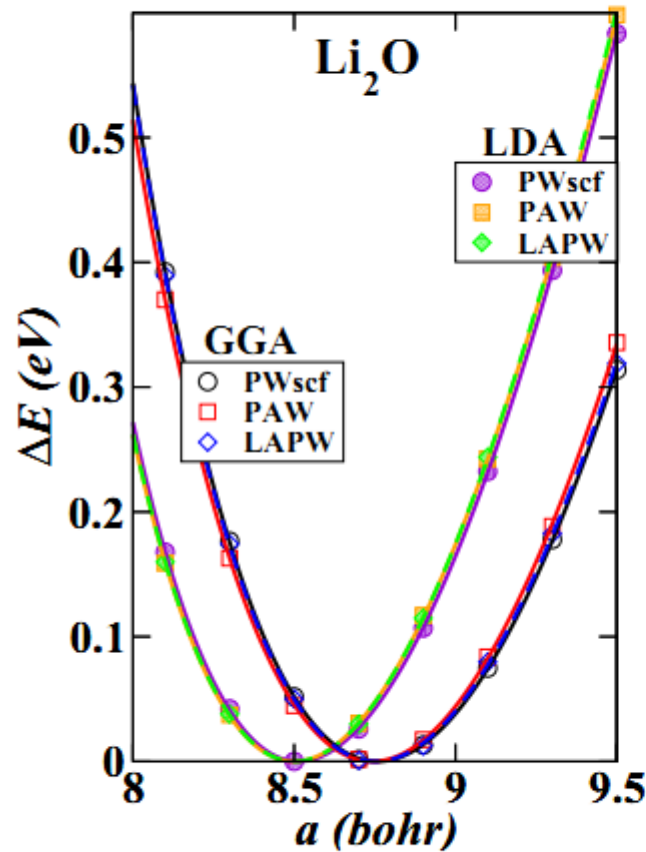
Holzwarth, Tackett, and Matthews, CPC 135 329 (2001) <http://pwpaw.wfu.edu>

Periodic Table of the Elements for PAW Functions

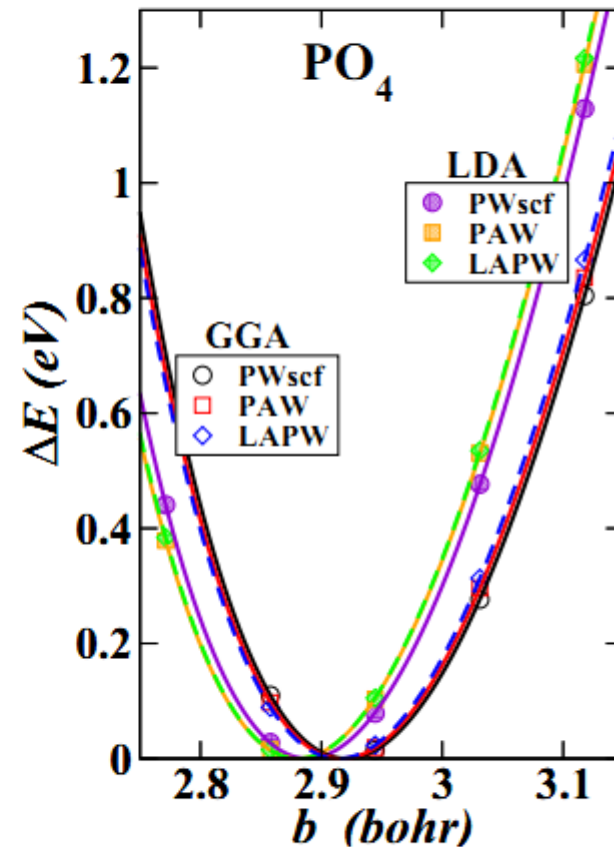
| | | | | | | | | | | | | | | | | | |
|----------|----------|----------|-----------|-----------|-----------|-----------|-----------|-----------|------------|------------|------------|----------|------------|-----------|------------|-----------|----------|
| 1 H | | | | | | | | | | | | | | | | | 2 He |
| 3 Li | 4 Be | | | | | | | | | | | 5 B | 6 C | 7 N | 8 O | 9 F | 10 Ne |
| 11 Na | 12 Mg | | | | | | | | | | | 13 Al | 14 Si | 15 P | 16 S | 17 Cl | 18 Ar |
| 19 K | 20 Ca | 21 Sc | 22 Ti | 23 V | 24 Cr | 25 Mn | 26 Fe | 27 Co | 28 Ni | 29 Cu | 30 Zn | 31 Ga | 32 Ge | 33 As | 34 Se | 35 Br | 36 Kr |
| 37 Rb | 38 Sr | 39 Y | 40 Zr | 41 Nb | 42 Mo | 43 Tc | 44 Ru | 45 Rh | 46 Pd | 47 Ag | 48 Cd | 49 In | 50 Sn | 51 Sb | 52 Te | 53 I | 54 Xe |
| 55 Cs | 56 Ba | | 72 Hf | 73 Ta | 74 W | 75 Re | 76 Os | 77 Ir | 78 Pt | 79 Au | 80 Hg | 81 Tl | 82 Pb | 83 Bi | 84 Po | 85 At | 86 Rn |
| 87 Fr | 88 Ra | | 104 Rf | 105 Db | 106 Sg | 107 Bh | 108 Hs | 109 Mt | 110 Uun | 111 Uuu | 112 Uub | | 114 Uuq | | 116 Uuh | | |
| | | 57 La | 58 Ce | 59 Pr | 60 Nd | 61 Pm | 62 Sm | 63 Eu | 64 Gd | 65 Tb | 66 Dy | 67 Ho | 68 Er | 69 Tm | 70 Yb | 71 Lu | |
| | | 89 Ac | 90 Th | 91 Pa | 92 U | 93 Np | 94 Pu | 95 Am | 96 Cm | 97 Bk | 98 Cf | 99 Es | 100 Fm | 101 Md | 102 No | 103 Lr | |

Datasets can interface with *abinit*, *quantum-espresso*, and other codes.

Test results for simple oxides

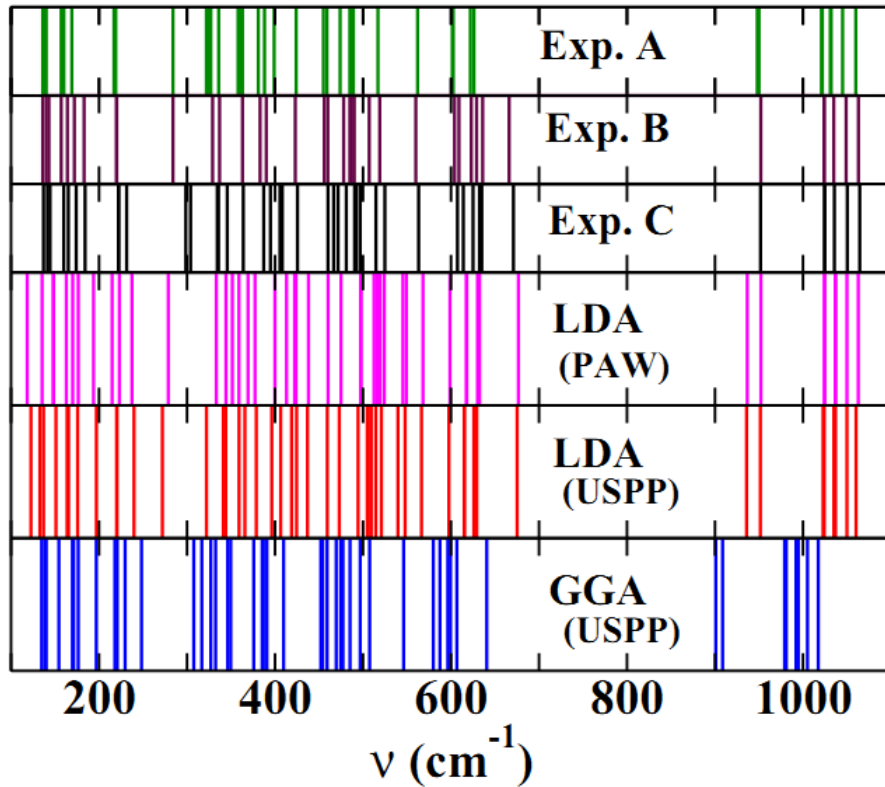


Fluorite structure

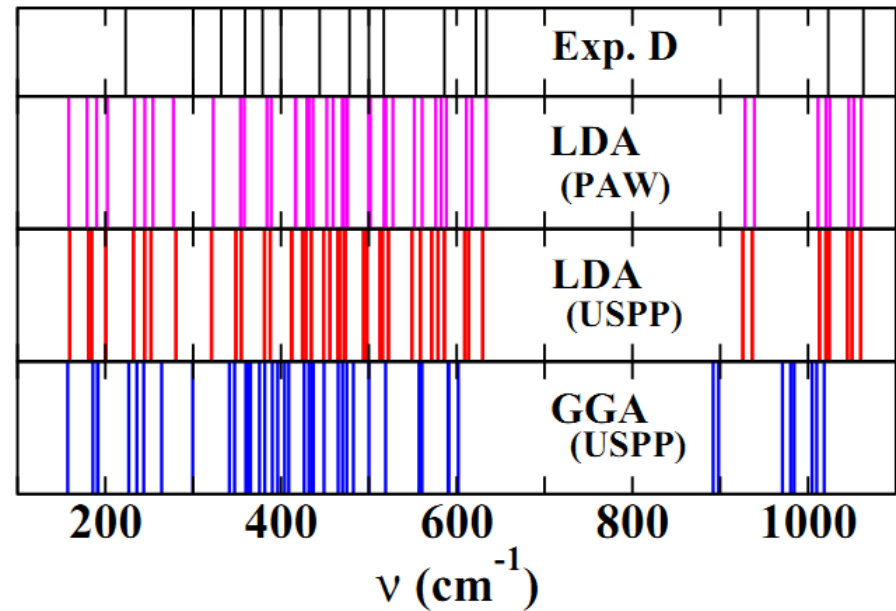


Tetrahedral molecule

Raman spectra – Experiment & Calculation

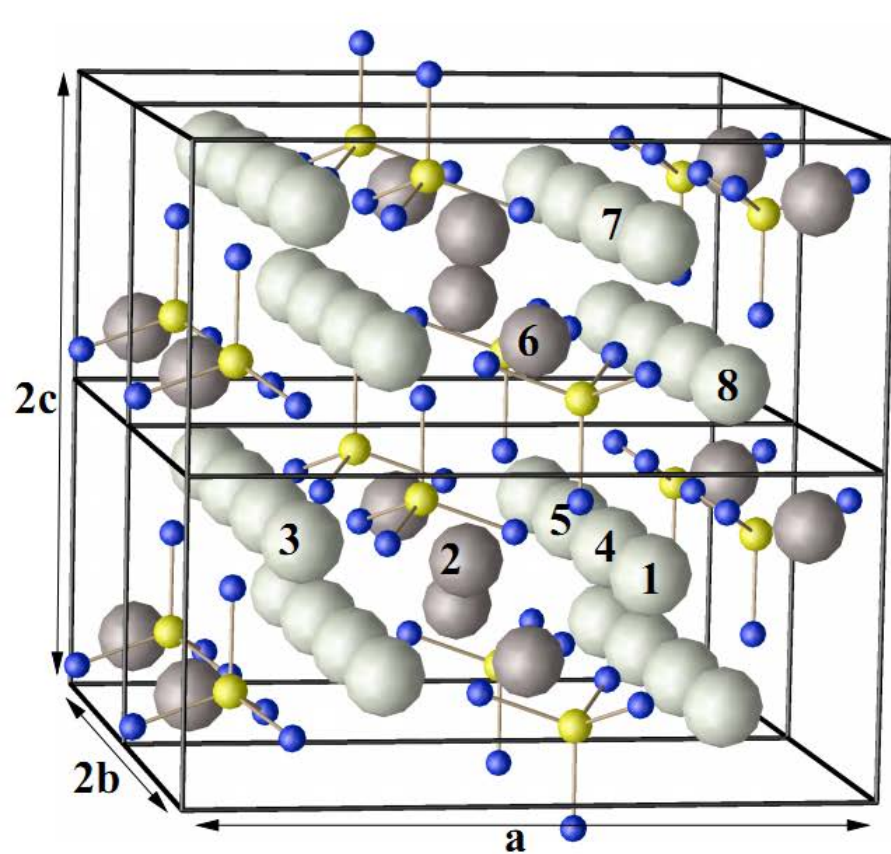


$\gamma\text{-Li}_3\text{PO}_4$

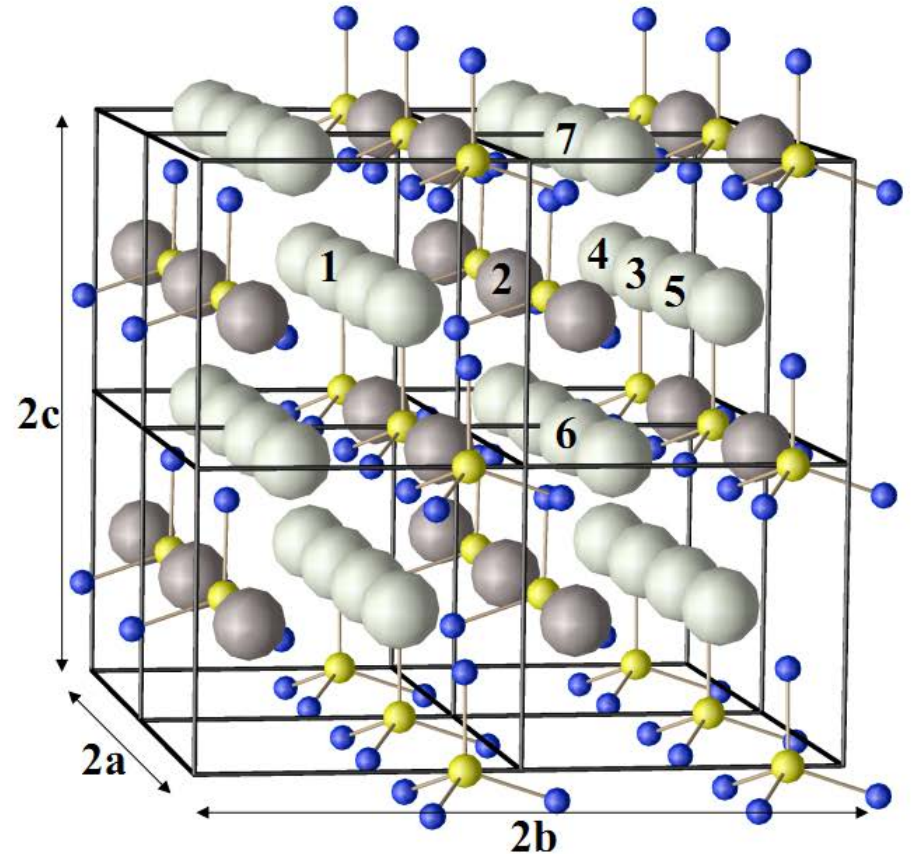


$\beta\text{-Li}_3\text{PO}_4$

Ball and stick models of Li_3PO_4 crystals



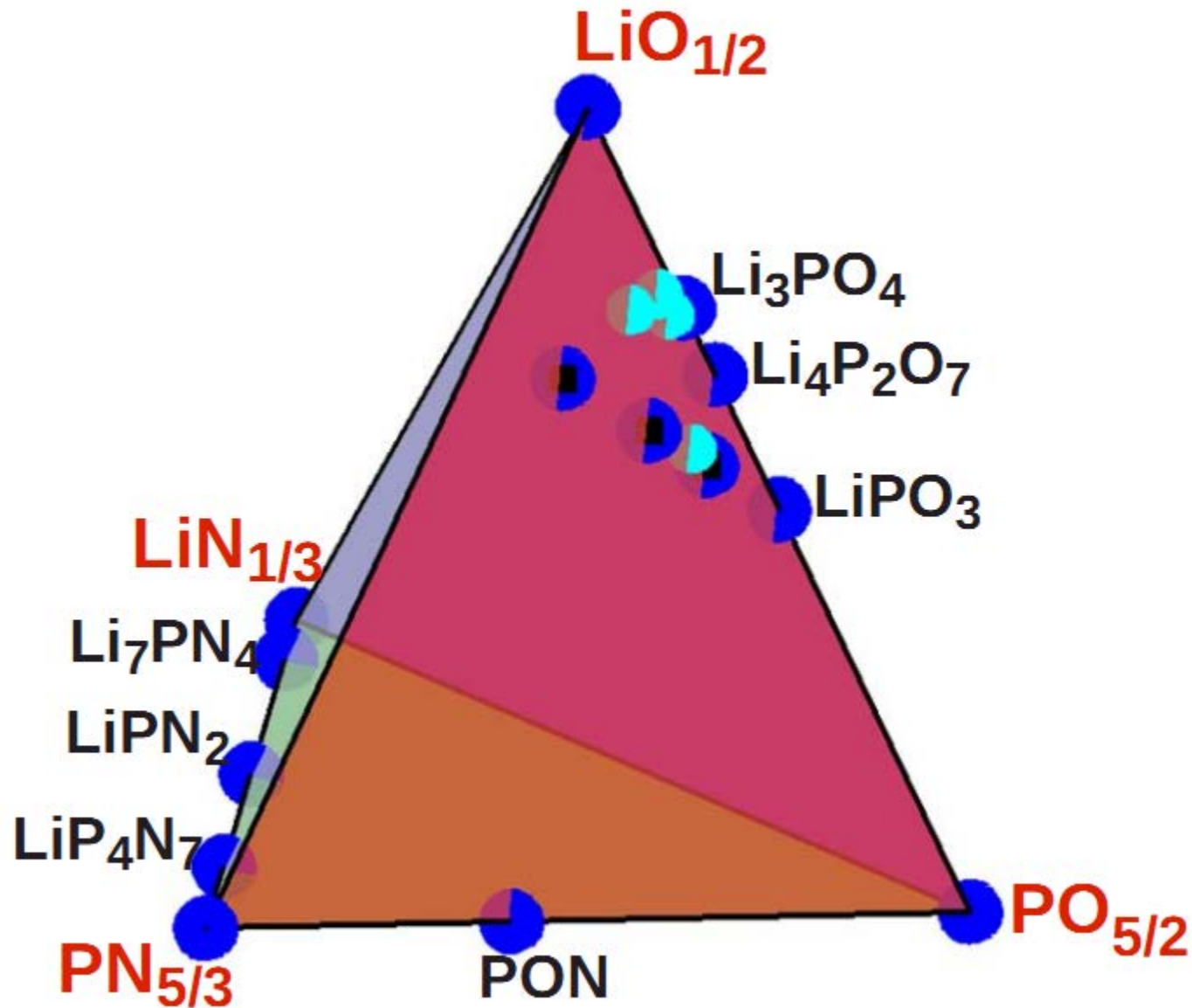
$\gamma\text{-Li}_3\text{PO}_4$



$\beta\text{-Li}_3\text{PO}_4$



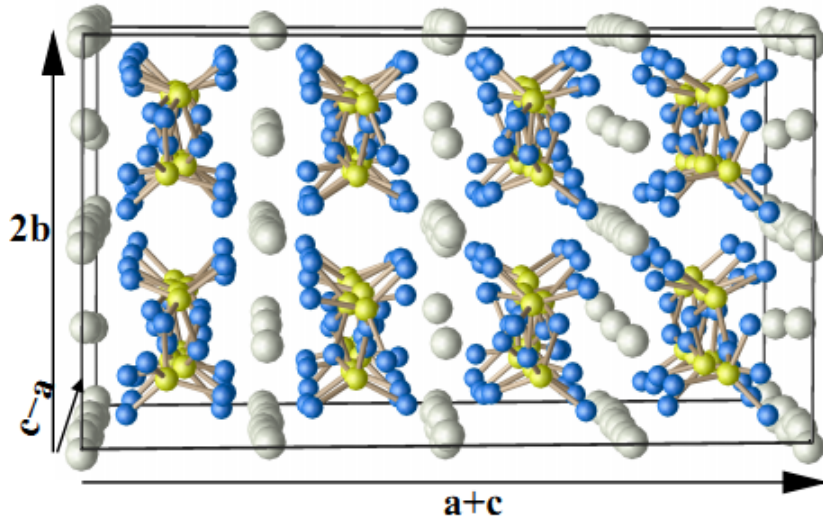
Systematic study of LiPON materials -- $\text{Li}_x\text{PO}_y\text{N}_z$



Phosphate chain materials: LiPO_3 plus N

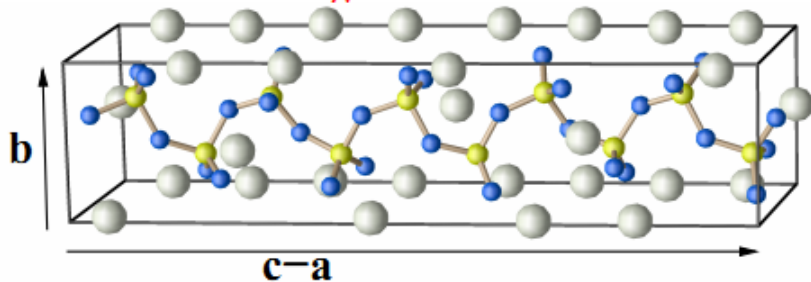
LiPO_3 in $P2/c$ structure; 100 atom unit cell

Chain direction perpendicular to plane of diagram



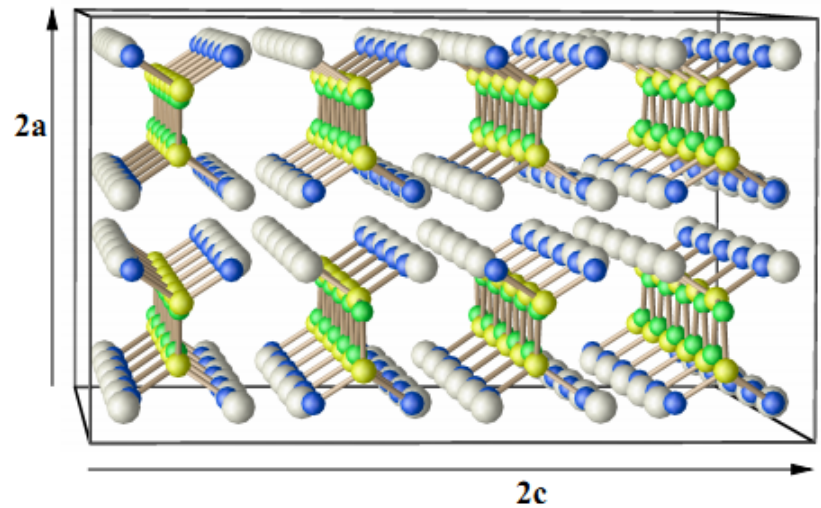
Ball colors: \bullet =Li, \bullet =P, \bullet =O.

Single chain view



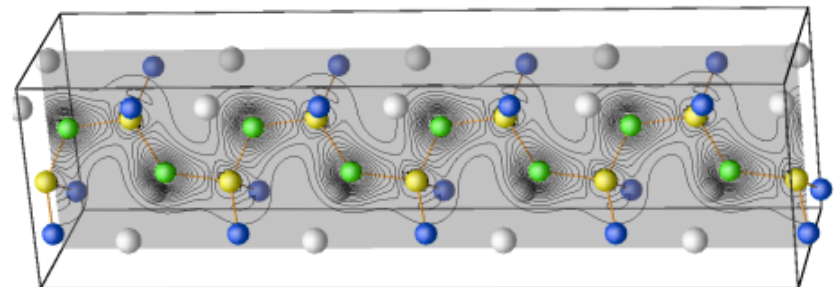
$s_1\text{-Li}_2\text{PO}_2\text{N}$ in $Pbcm$ structure; 24 atom unit cell

Chain direction perpendicular to plane of diagram

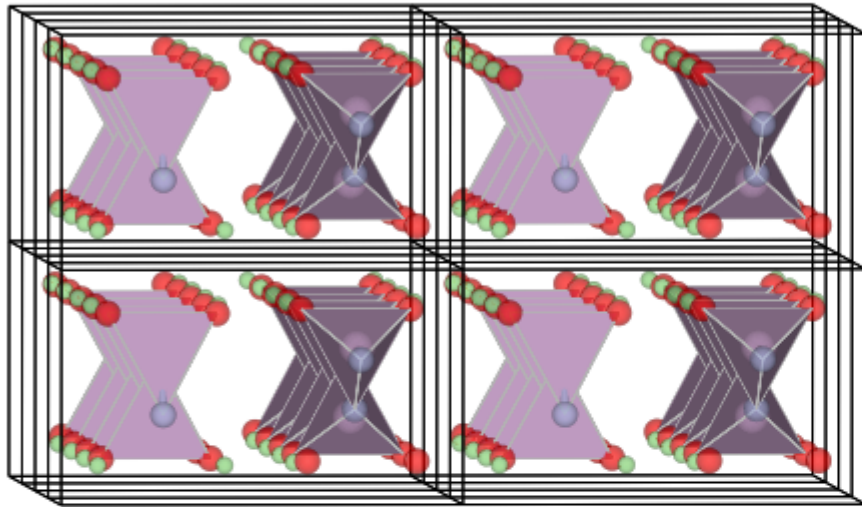


Ball colors: \bullet =Li, \bullet =P, \bullet =O, \bullet =N.

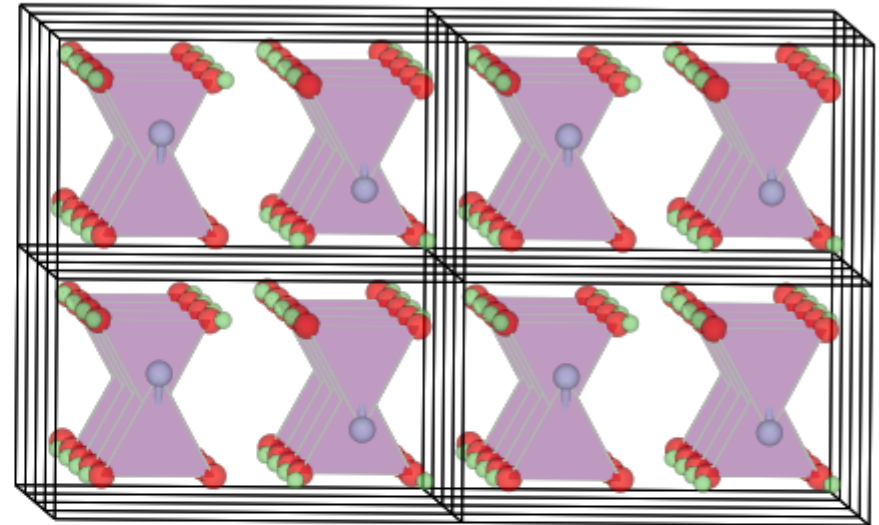
Single chain view



Two forms of $\text{Li}_2\text{PO}_2\text{N}$

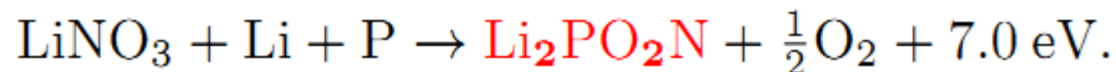
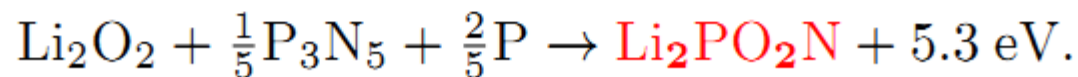
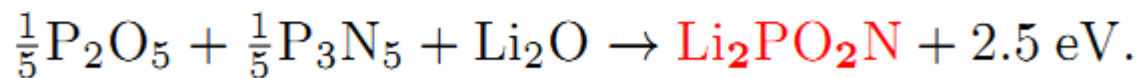


$s_1\text{-Li}_2\text{PO}_2\text{N}$



$s_2\text{-Li}_2\text{PO}_2\text{N}$

Possible exothermic reaction pathways:



Summary of measured and calculated conductivity parameters in $\text{Li}_x\text{PO}_y\text{N}_z$ materials

Measured activation energies E_A^{exp} compared with calculated migration energies for vacancy (E_m^{cal} (vac.)) and interstitial (E_m^{cal} (int.)) mechanisms and vacancy-interstitial formation energies (E_f^{cal}). All energies are given in eV.

| Material | Form | E_A^{exp} | E_m^{cal} (vac.) | E_m^{cal} (int.) | E_f^{cal} | E_A^{cal} |
|---|-----------------------------|--------------------|---------------------------|---------------------------|--------------------|--------------------|
| $\gamma\text{-Li}_3\text{PO}_4$ | single crystal ^a | 1.23, 1.14 | 0.7, 0.7 | 0.4, 0.3 | 1.7 | 1.3, 1.1 |
| $\text{Li}_{2.88}\text{PO}_{3.73}\text{N}_{0.14}$ | poly cryst. | 0.97 | | | | |
| $\text{Li}_{3.3}\text{PO}_{3.9}\text{N}_{0.17}$ | amorphous | 0.56 | | | | |
| $\text{Li}_{1.35}\text{PO}_{2.99}\text{N}_{0.13}$ | amorphous | 0.60 | | | | |
| LiPO_3 | poly cryst. | 1.4 | 0.6, 0.7 | 0.7 | 1.2 | 1.1-1.2 |
| LiPO_3 | amorphous | 0.76-1.2 | | | | |
| $s_1\text{-Li}_2\text{PO}_2\text{N}$ | single crystal | | 0.5, 0.6 | | 1.7 | 1.3-1.5 |
| LiPN_2 | poly cryst. | 0.6 | 0.4 | | 2.5 | 1.7 |
| Li_7PN_4 | poly cryst. | 0.5 | | | | |

Other electrolyte materials -- thiophosphate

LiPON and $\text{LiS}_2\text{-P}_2\text{S}_5$ conductivities

X. Yu, J. B. Bates, G. E. Jellison, Jr., and F. X. Hart, J. Electrochem. Soc. **144** 524-532 (1997):

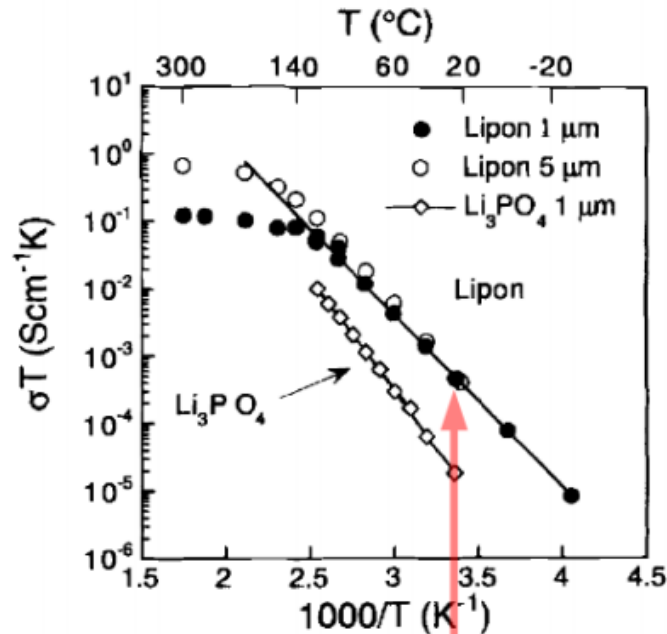


Fig. 3. Arrhenius plot of ionic conductivity of Lipon and Li_3PO_4 vs. temperature.

$$\sigma = 2 \times 10^{-6} \text{ S/cm}$$

$$E_a = 0.5 \text{ eV}$$

M. Tatsumisago and A. Hayashi, J. Non-Cryst. Solids **354** 1411-1417 (2008):

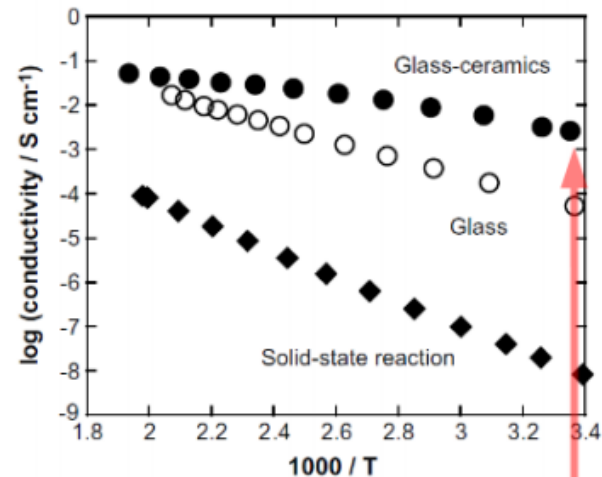
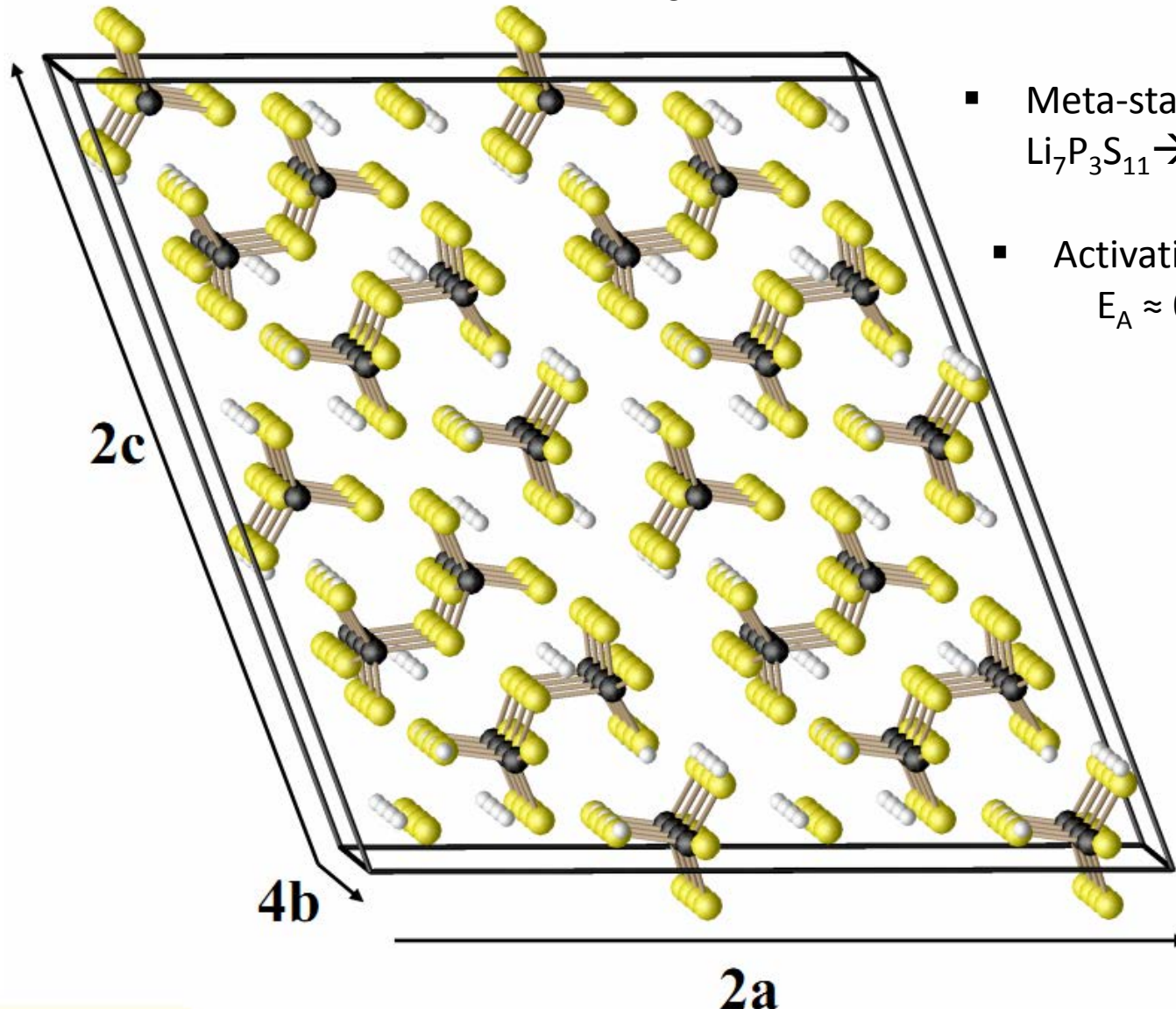


Fig. 5. Temperature dependences of the conductivities for the $70\text{Li}_2\text{S} \cdot 30\text{P}_2\text{S}_5$ glass and glass-ceramics. The conductivity data for the sample prepared by solid-state reaction are also shown.

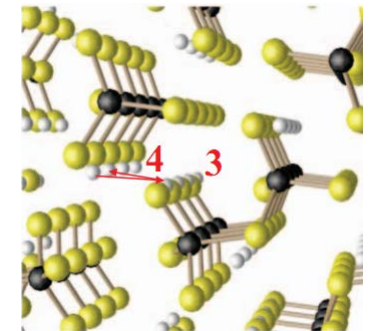
$$\sigma = 3 \times 10^{-3} \text{ S/cm}$$

$$E_a = 0.1 \text{ eV}$$

“Superionic conductor” $\text{Li}_7\text{P}_3\text{S}_{11}$



- Meta-stable to decomposition:
 $\text{Li}_7\text{P}_3\text{S}_{11} \rightarrow \text{Li}_3\text{PS}_4 + \text{Li}_4\text{P}_2\text{S}_6 + \text{S}$
- Activation energy estimate:
 $E_A \approx 0.2 \text{ eV}$ (Exp. 0.1 eV)



- Interstitial-vacancy pair formation energy $E_f \approx 0$

Yamane et al, *Solid State Ionics* **178** 1163 (2007)

Other simulation studies on this material:

Work by MIT group published in Dec. 2011

CHEMISTRY OF
MATERIALS


Communication

pubs.acs.org/cm

First Principles Study of the Li₁₀GeP₂S₁₂ Lithium Super Ionic Conductor Material

Yifei Mo, Shyue Ping Ong, and Gerbrand Ceder*

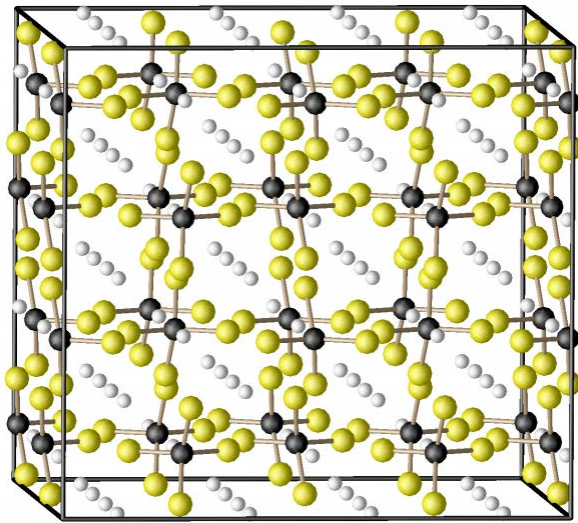
Department of Materials Science and Engineering, Massachusetts Institute of Technology, Cambridge, Massachusetts 02139, United States

 Supporting Information

KEYWORDS: *lithium ionic conductor, solid electrolyte, Li₁₀GeP₂S₁₂, ab initio, molecular dynamics, phase diagrams*

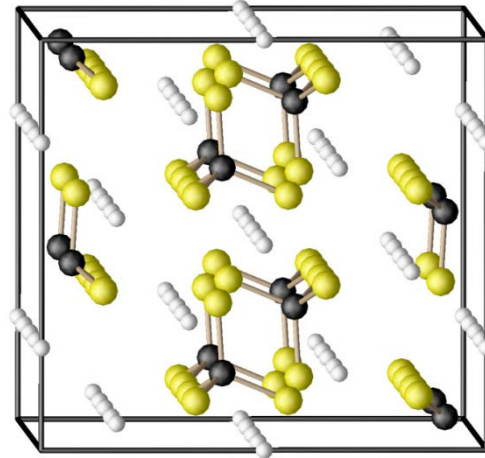
dx.doi.org/10.1021/cm203303y | Chem. Mater. 2012, 24, 15–17

Constituents of $\text{Li}_{10}\text{GeP}_2\text{S}_{12}$:



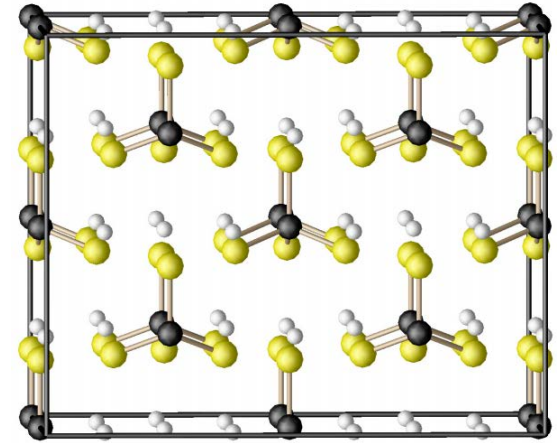
$\alpha^* - \text{Li}_3\text{PS}_4$ *Pbcn*

$\Delta H = -8.12 \text{ eV}$



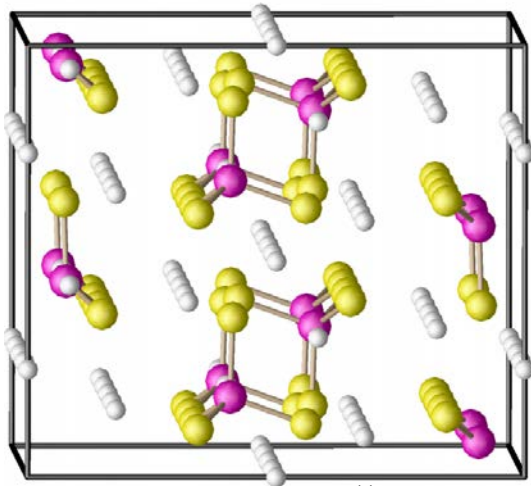
$\beta^* - \text{Li}_3\text{PS}_4$ *Pnma*

$\Delta H = -8.28 \text{ eV}$



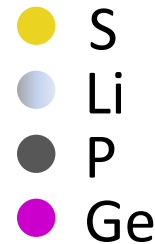
$\gamma^* - \text{Li}_3\text{PS}_4$ *Pmn2_1*

$\Delta H = -8.36 \text{ eV}$



Li_4GeS_4 *Pnma^{**}*

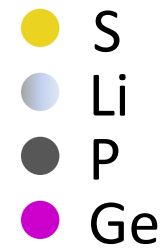
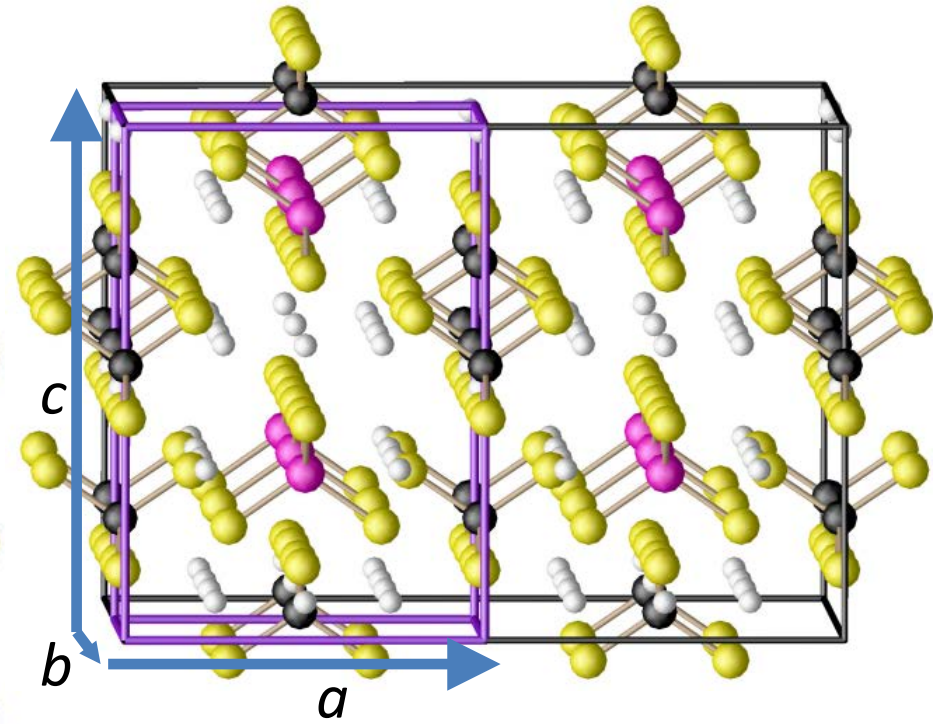
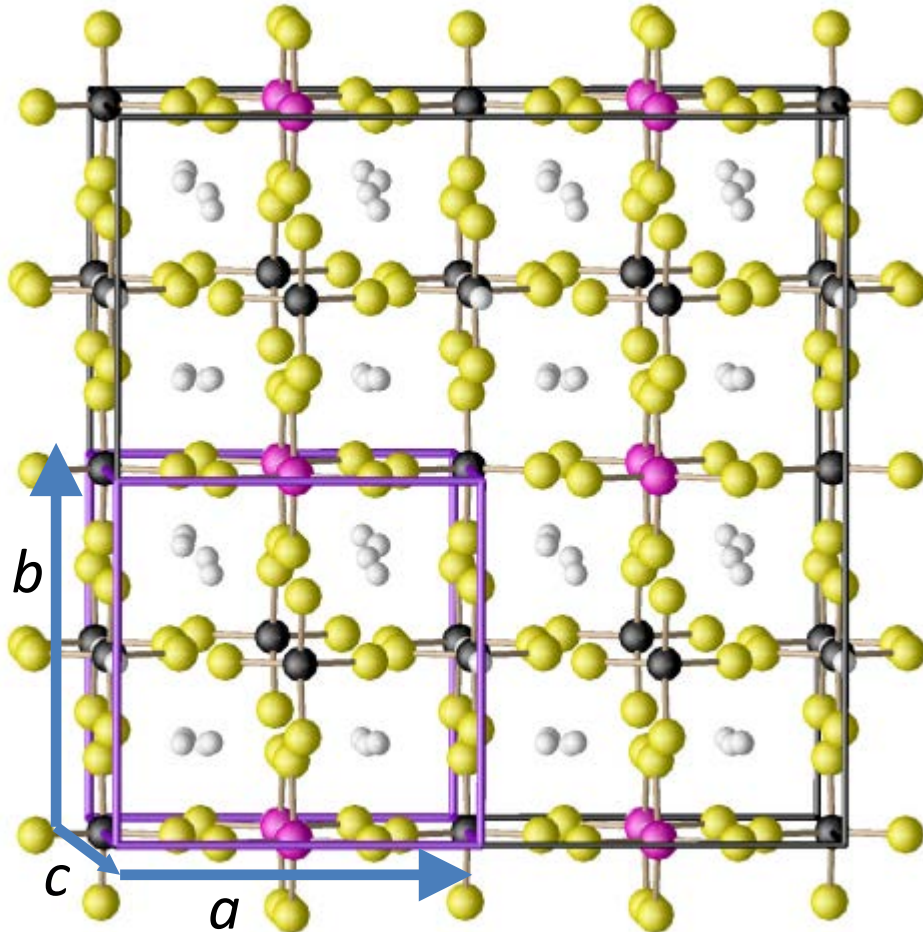
$\Delta H = -10.19 \text{ eV}$



*K. Homma et al, *Solid State Ionics* **182**, 53-58 (2011)

M. Murayama et al, *Solid State Ionics* **154-155, 789-794 (2002)

$\text{Li}_{10}\text{GeP}_2\text{S}_{12}$
Space group $P4_2/nmc$ (#137)
(from experiment)



| | a (Å) | c (Å) |
|--|---------|---------|
| $\text{Li}_{10}\text{GeP}_2\text{S}_{12}$ (exp*) | 8.72 | 12.63 |
| $\text{Li}_{10}\text{GeP}_2\text{S}_{12}$ (Calc) | 8.56 | 12.23 |
| $\text{Li}_{10}\text{SiP}_2\text{S}_{12}$ (Calc) | 8.55 | 12.16 |

*Kamaya et al, *Nature Materials* **10**, 682-686 (2011)

Experimentally determined symmetry (fractional occupancy):

Space group $P4_2/nmc$ (#137)

Optimized structure with full occupancy:*

Space group $P4_2mc$ (#105)

$$(x, y, z) \rightarrow (y, x, -z)$$

*Determined using FINDSYM written by Stokes, Campbell, and Hatch at Brigham Young U. –

<http://stokes.byu.edu/iso/>

Experiment structure:

Space group $P4_2/nmc$ (#137)

| Atom | <i>g</i> | <i>x</i> | <i>y</i> | <i>z</i> |
|-----------|----------|----------|----------|----------|
| Li(1) 16h | 0.69 | 0.26 | 0.27 | 0.18 |
| Li(2) 4d | 1.00 | 0.00 | 0.50 | 0.94 |
| Li(3) 8f | 0.64 | 0.25 | 0.25 | 0.00 |
| Ge(1) 4d | 0.52 | 0.00 | 0.50 | 0.69 |
| P(1) 4d | 0.49 | 0.00 | 0.50 | 0.69 |
| Ge(2) 2b | 0.00 | 0.00 | 0.00 | 0.50 |
| P(2) 2b | 1.00 | 0.00 | 0.00 | 0.50 |
| S(1) 8g | 1.00 | 0.00 | 0.18 | 0.41 |
| S(2) 8g | 1.00 | 0.00 | 0.30 | 0.10 |
| S(3) 8g | 1.00 | 0.00 | 0.70 | 0.79 |

Calculated structure:

Space group $P4_2mc$ (#105)*

| Atom | <i>g</i> | <i>x</i> | <i>y</i> | <i>z</i> |
|-------------|----------|----------|----------|----------|
| Li(1) 8f | 1.00 | 0.23 | 0.23 | 0.29 |
| Li(2) 2a/2b | 1.00 | 0.00 | 0.50 | 0.94 |
| Li(3) 8f | 1.00 | 0.26 | 0.22 | 0.03 |
| Ge(1) 2b | 1.00 | 0.50 | 0.00 | 0.79 |
| P(1) 2a | 1.00 | 0.00 | 0.50 | 0.68 |
| | | | | |
| P(2) 2c | 1.00 | 0.00 | 0.00 | 0.50 |
| S(1) 4d/4e | 1.00 | 0.00 | 0.20 | 0.41 |
| S(2) 4d/4e | 1.00 | 0.00 | 0.30 | 0.09 |
| S(3) 4d/4e | 1.00 | 0.00 | 0.70 | 0.78 |

*Wyckoff symbols for #105, coordinates in #137 convention.

Decomposition reactions predicted on the basis of calculated enthalpies of formation (at zero temperature)

| | ΔH (eV) |
|---|-----------------|
| $\text{Li}_{10}\text{GeP}_2\text{S}_{12} \rightarrow 2\text{Li}_3\text{PS}_4 + \text{Li}_4\text{GeS}_4$ | 0.77 |
| $\text{Li}_{10}\text{SiP}_2\text{S}_{12} \rightarrow 2\text{Li}_3\text{PS}_4 + \text{Li}_4\text{SiS}_4$ | 0.74 |
| $\text{Li}_{13}\text{GeP}_3\text{S}_{16} \rightarrow 3\text{Li}_3\text{PS}_4 + \text{Li}_4\text{GeS}_4$ | 0.55 |
| $\text{Li}_{13}\text{SiP}_3\text{S}_{16} \rightarrow 3\text{Li}_3\text{PS}_4 + \text{Li}_4\text{SiS}_4$ | 0.62 |

➔ Preliminary results for formation enthalpies from zero-temperature simulations predict all of the compounds to be unstable with respect to their constituents.

➔ Work continuing to investigate Li ion migration energies.

Summary and conclusions

- Ideal research effort in materials includes close collaboration of both simulations and experimental measurements.
- For battery technology, there remain many opportunities for new materials development.
- Case studies carried out by our group for solid electrolyte materials including Li phosphorus oxinitrides, Li thiophosphates, and very preliminary results for materials containing thiogerminates.

Some workshops for “first-principles” public domain codes

- WIEN2k Workshop 9/3/2012 Tokyo, Japan
- Quantum Espresso Workshop 6/25/2012 Penn State U.